

Contract No. and Disclaimer:

This manuscript has been authored by Savannah River Nuclear Solutions, LLC under Contract No. DE-AC09-08SR22470 with the U.S. Department of Energy. The United States Government retains and the publisher, by accepting this article for publication, acknowledges that the United States Government retains a non-exclusive, paid-up, irrevocable, worldwide license to publish or reproduce the published form of this work, or allow others to do so, for United States Government purposes.

Backscatter Gauge Description

for

Inspection of Neutron Absorber Uniformity and Content

Savannah River National Laboratory
Analytical Development and Research and Development Engineering
Imaging and Radiation Systems
R. A. Dewberry, K. M. Gibbs, and
A. H. Couture.

Abstract

This paper describes design, calibration, and testing of a dual He-3 detector neutron backscatter gauge for use in the Savannah River Site Mixed Oxide Fuel project. The gauge is demonstrated to measure boron content and uniformity in concrete slabs used in the facility construction.

Introduction

The Savannah River National Laboratory (SRNL) was requested by the Mixed Oxide Fuel (MOX) project to provide a gauge to measure boron content in concrete. At the MOX facility, boron will be added to the concrete moderator and shielding used in the facility in order to reduce and manage neutron flux. The requested gauge is to measure boron content and uniformity in concrete slabs used in the facility construction. Among candidate gauges to measure boron content the authors considered γ -ray spectroscopy to measure ^{10}B content using the $^{10}\text{B}(\text{n},\gamma)^{11}\text{B}$ reaction as well as the $^{10}\text{B}(\text{n},\alpha)^7\text{Li}$ reaction and neutron backscatter. After scoping experiments in our nuclear nondestructive assay facility, the authors selected the backscatter probe. This paper describes development, testing, and calibration of our composite gauge.

The conceptual design of our neutron backscatter gauge is similar to that used by the Troxler moisture gauge of reference 1 and to several additional transmission and backscatter neutron gauges of references 2 – 5. The Bastruk JEN-3 gauge⁽²⁾ and the Korkut gauge⁽⁴⁾ relate boron content in stainless steel and colmanite cement using neutron transmission. The TSAO gauge uses neutron backscatter in a single-detector gauge to probe for discontinuities of absorber content with under-moderated neutrons.⁵ Our gauge design is shown in a conceptual diagram in Figure 1 and is described thoroughly in the invention disclosure of reference 6. It consists of an encapsulated neutron source located in the center of the gauge. The source is surrounded by a polyethylene cylinder. This cylinder slows the neutrons to thermal or near-thermal so they can be absorbed by the cadmium foil which wraps the cylinder. This foil (plus an additional 2mm Cd disk on top of the source not shown in Figure 1) protects the neutron detectors from observing neutrons coming directly from the source. The bottom of the polyethylene cylinder is open to allow the neutrons to freely enter the concrete component to be inspected for boron content.

The neutrons that enter the concrete may backscatter toward the gauge where they can be detected by the neutron detectors. The neutron detectors are embedded in ultra-high molecular weight (UHMW) polyethylene slabs whose function is to lower the energy of the backscattered neutrons so they can be detected with higher efficiency. Two detectors are used with the source in the middle so that the gauge will provide a symmetric response. That is, with the single detector used in the gauges of 1 – 5, a different response would be obtained near edges of the observed component depending on whether the source or detector is closer to the edge. A thin aluminum (Al) “scuff” plate is included to prevent damage to the polyethylene slabs. Al is essentially transparent to the

neutrons. The outside dimensions of the probe are 9.5 inch x 9.5 inch with a height of 1.25 inch.

The gauge functions on the principle that energetic neutrons from the Am(Li) (α ,n) reaction are exposed to the boron-containing concrete slab. A large fraction of these neutrons are then scattered back toward the gauge, where they are moderated to near thermal by the polyethylene and detected by the dual He-3 detectors. For concrete with no boron (or other neutron absorber) the backscatter detection rate will be N_0 . With non-zero boron content the backscatter flux and detection rate is reduced. Therefore the backscatter detection rate will be inversely related to boron content and can likely be modeled with the empirical exponential form

$$\text{Detection rate} = N_0 \exp(-C[B]), \quad (1)$$

where $[B]$ represents known boron content in the observed cement component, and N_0 and C are constants to be determined.

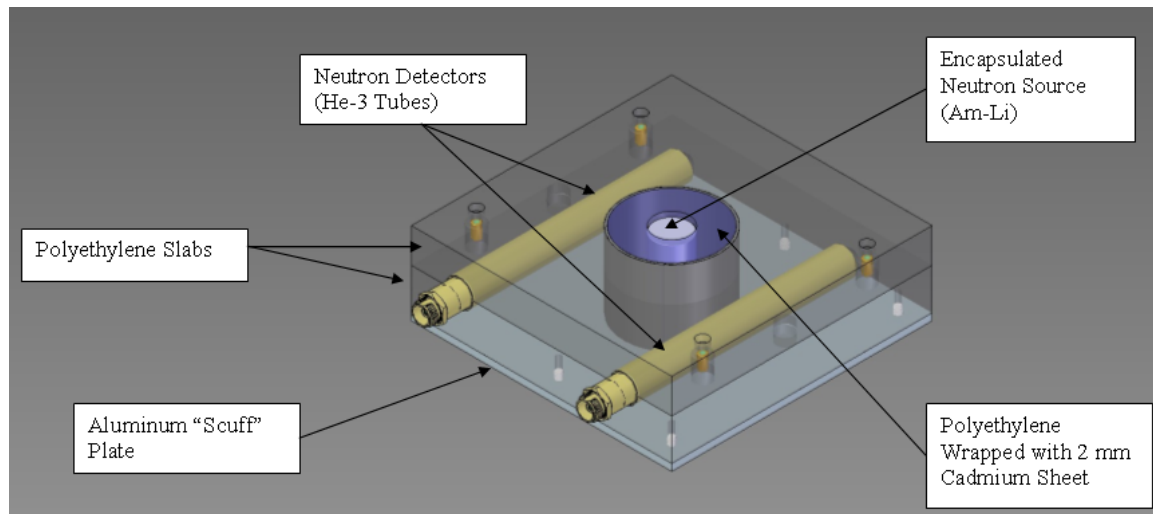


Figure 1: Conceptual design of the neutron gauge.

Detailed Gauge Description

The gauge consists primarily of the neutron source, neutron detectors, detector pulse counting electronics, and moderator assembly. The source is an Americium/Lithium (Am-Li) neutron source with an initial α -decay activity of 1.2 Curie and a neutron emission rate of 50,000 neutrons per second into a 4π geometry. The (α ,n) neutron energy spectrum is approximately reproduced in Figure 2.⁷

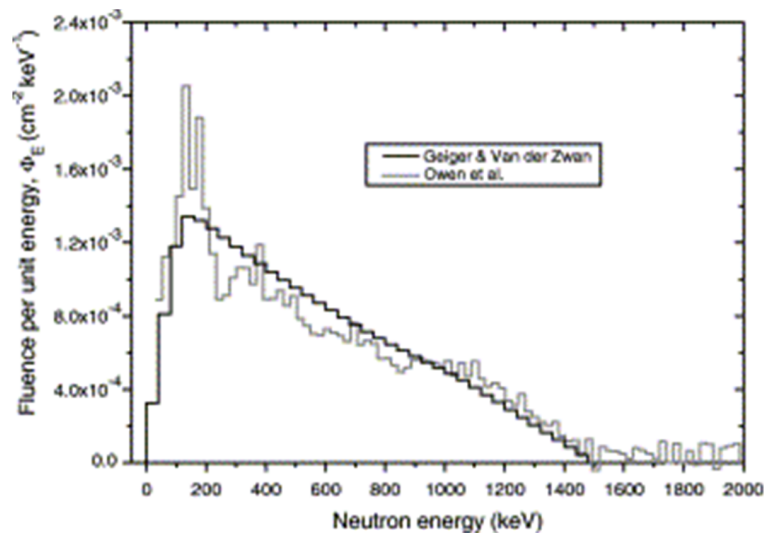


Figure 2: The $^{241}\text{Am-Li}$ radionuclide neutron source spectrum [2].

The gauge contains two Reuter-Stokes model RS-P4 He-3 type neutron detectors. This detector design is a gas filled (He-3) steel tube 1 inch in diameter and with an effective length of 8 inches. The helium gas pressure is 4 atm. The two specific detectors were selected to have matching regions of proportional counting near 1500 volts determined by experiment.

The detector pulse counting electronics consist of Reuter-Stokes 122A pre-amplifiers, a Canberra 2015A AMP/SCA, and a Jomar JSR-11 high voltage supply and shift register to count neutron singles, doubles, and accidentals. These components were connected as shown in Figure 3. Note the dual detectors are set up in tandem so that they are driven by the same HV supply. Similarly the detector analog output of one passes through the other before being combined as a single signal going to amp/SCA. The SCA out from the 2015A module is then fed to the JSR-11 input for analysis of the TTL event rate.

The analog *preamp out* signals are approximately 5mV in amplitude with negative polarity. With suitable amplification we were able to generate a multichannel analyzer (MCA) spectrum expected for properly operating neutron tubes.⁸ The tandem counting configuration allows the shift register to analyze the event rate as a single chain as almost all neutron counting configurations are devised.

In our initial testing with both the Am(Li) source and with a 7.9-g Pu-239,240 source we obtained event rates with the detectors combined in tandem and also disconnected to operate as a single unit in order to demonstrate we had obtained proper summing of the TTL rates. We do not include these data in this paper. Using the Pu source and with a 64- μsec coincidence gate, we also demonstrated the capability of the shift register to observe coincidence neutron events. Like the generation of the MCA spectrum above, observing this neutron coincidence rate is not an important component for use of our

The diagram illustrates the electrical connections for the JOMAR JSR-II Counter/High Voltage Supply. The supply unit is connected to three main components:

- 4006 MINIBIN:** The HV (High Voltage) output of the supply is connected to the MINIBIN. The SCA OUT (Single Channel Analyzer Output) is connected to the AMP IN (Amplifier Input) of the REUTER STOKES 122A PREAMP.
- REUTER STOKES 122A PREAMP:** This preamplifier is connected to two He-3 Tubes. The DET IN (Detector Input) is connected to the HV output of the supply. The DET OUT (Detector Output) is connected to the SCA/AMP 2015A.

A note specifies: "NOTE: SET SCA FOR (-) POLARITY PULSE". The entire setup is labeled "GAUGE BLOCK AND NEUTRON SOURCE".

Experimental

Panel S/N	Boron Content (g/cm³)
100-A	0.189
100-B	0.189
80	0.151
50	0.095
20	0.038

One acquisition was obtained in the center of each slab, and one was obtained at each of the four corners. The corner samples were taken with the detector centered at approximately 15 cm from the corners. Three trials were made at each of the five sample points for a total of 15 measurements per panel. The five distinct measurements locations allowed us to demonstrate uniformity for each individual panel and to demonstrate whether our gauge design is successful to eliminate edge effects. The three acquisitions at each measurement location yielded precision of the instrument.

A Monte Carlo neutron calculation⁹ demonstrated to us that approximately 30% of the Am(Li) source neutrons are able to completely penetrate through the 5-cm panels and that approximately 65% would be backscattered off of the cement with no boron loading. According to the MCNP modeling with variable loading of boron up to 0.189 g/cm³, backscatter will be degraded with an exponential relationship by increasing boron content. The model is consistent with equation (1).

Our experimental measurements also included measure of neutron backscatter in air and off of the tiled cement floor of the laboratory facility. We treated the backscatter in air as our background. The floor backscatter measurements approximately represented null boron loading concrete, though we believe much less than 30% of the Am(Li) neutrons were able to completely penetrate the entire floor thickness.

Results

A thorough presentation of measurement results as well as a thorough statistical analysis of the measurements appears in reference 10. We include in Table 2 all of the measurements obtained on panel 100-A to demonstrate the instrumental precision (triplicate acquisitions at each point) and the panel uniformity (acquisition location). We then present in Table 3 the average values of all fifteen acquisitions for each panel without the stainless steel plate. In Table 4 we present the same values with the stainless steel plate between the panel and the gauge.

Table 2: Raw data from panel S/N 100-A (100%), 70 second count time.

Grid Pt.	Trial 1	Trial 2	Trial 3		Pt. Avg.
1	87310	87525	87584		87473
2	87279	87669	87784		87577
3	87167	88030	87505		87567
4	87283	87595	87488		87455
5	87779	88294	87724		87932
Avg.	87601.07			Avg.	87600.80
Std. Dev	299.42			Std. dev.	193.00

Table 3. Bare ConcreteAvg. Counts vs. Loading, 70 second Count Time.

Boron Loading (g/cc)	Avg. Raw Counts	Air Counts	Net Count
0.189	87601.07	76670.00	10931.07
0.189	87662.60	76670.00	10992.60
0.151	88266.80	76670.00	11596.80
0.095	89282.80	76670.00	12612.80
0.038	91363.60	76670.00	14693.60
0	101646.20	76670.00	24976.20

Table 4. SS(3mm) Clad Concrete Avg. Counts vs. Loading, 70 second Count Time

Boron Loading (g/cc)	Avg. Raw Counts	Air Counts	Net Count
0.189	89800.4	76670.00	13130.40
0.189	89838.6	76670.00	13168.60
0.151	90156.8	76670.00	13486.80
0.095	90844.6	76670.00	14174.60
0.038	92854	76670.00	16184.00

The results in Tables 3 are plotted in Figure 4 demonstrating the exponential relationship between backscatter detection rate and boron content. In the experiment we have exchanged the coordinates compared to the MCNP model. The relationship without the stainless steel plate is predicted by equation (2).

$$y = 22.34\exp(-0.03037x), \quad (2)$$

where x is (measured net counts/sec) and y is boron loading in units of g/cc. The relationship with the stainless steel plate (Figure 5) is predicted by

$$y = 206.9\exp(-0.03744x). \quad (3)$$

On both figures we designate the three-sigma uncertainty limits. In identical calibration measurements with the Troxler gauge, the three-sigma limits are much wider due to the lower source strength, single detector, lack of moderation, and asymmetry.

Inserting the laboratory floor (zero loading) detection rate of 24976 counts/70-sec yields a loading of less than 0.0005 g/cc for either equation (2) or (3). The extremely good precision of our acquisitions indicates 0.001 g/cc loading is a realistic sensitivity limit for the technique. Neither of (2) or (3) becomes excessively steep as we approach zero detected neutron events. That is, their first derivatives are finite and negative for all values down to $x = 0$, and both equations yield realistic calculations of boron content

within extrapolated detection uncertainties. We believe both equations can be considered valid up to an arbitrary limit of approximately 0.25 g B/ cm³. ~~However we do not have the data to validate that limit.~~

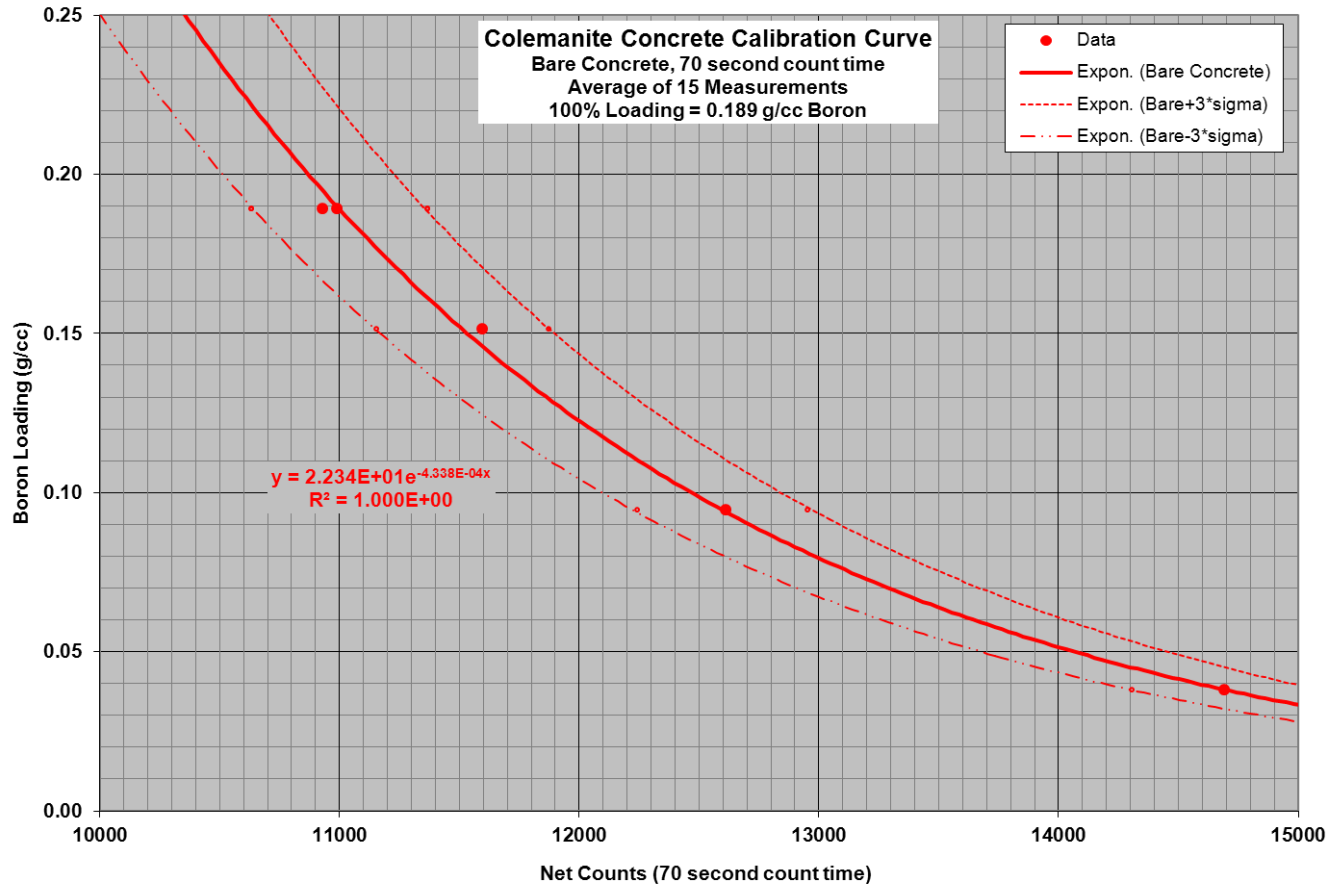


Figure 4. Bare Colemanite concrete calibration curve.

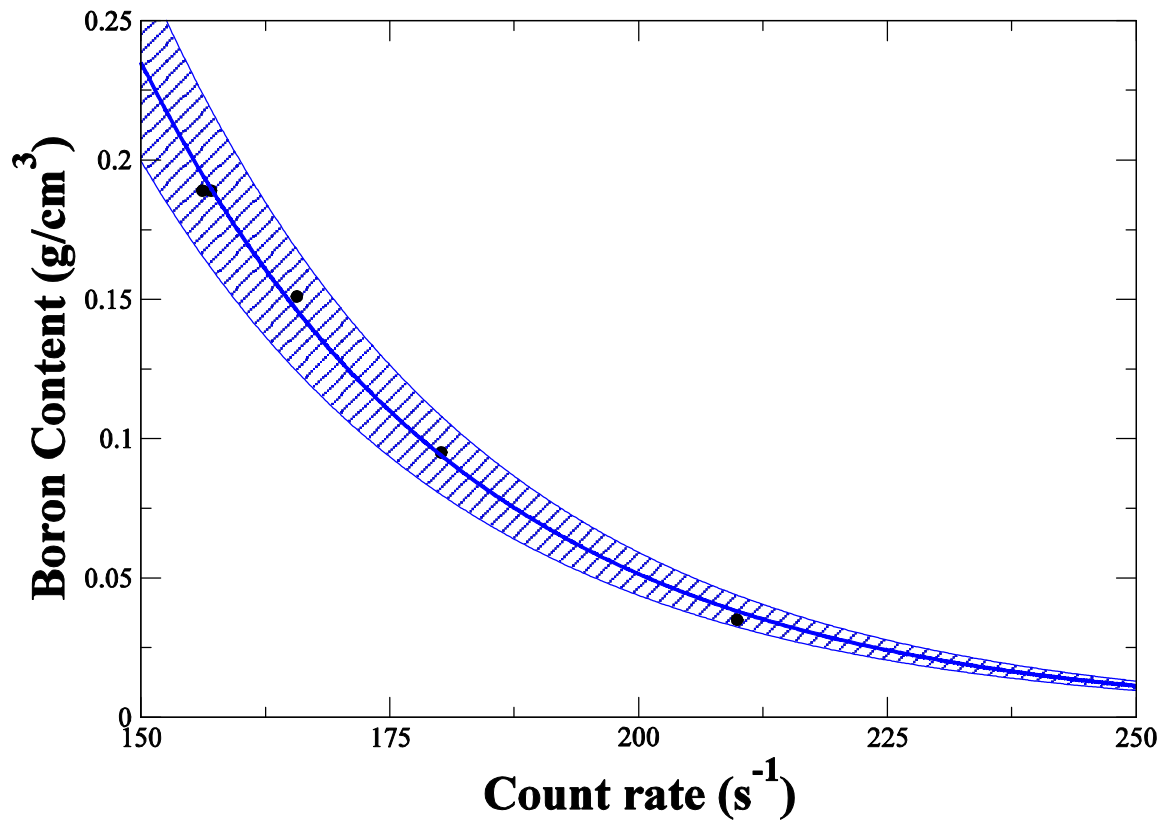


Figure 4. Bare Colemanite concrete calibration curve.

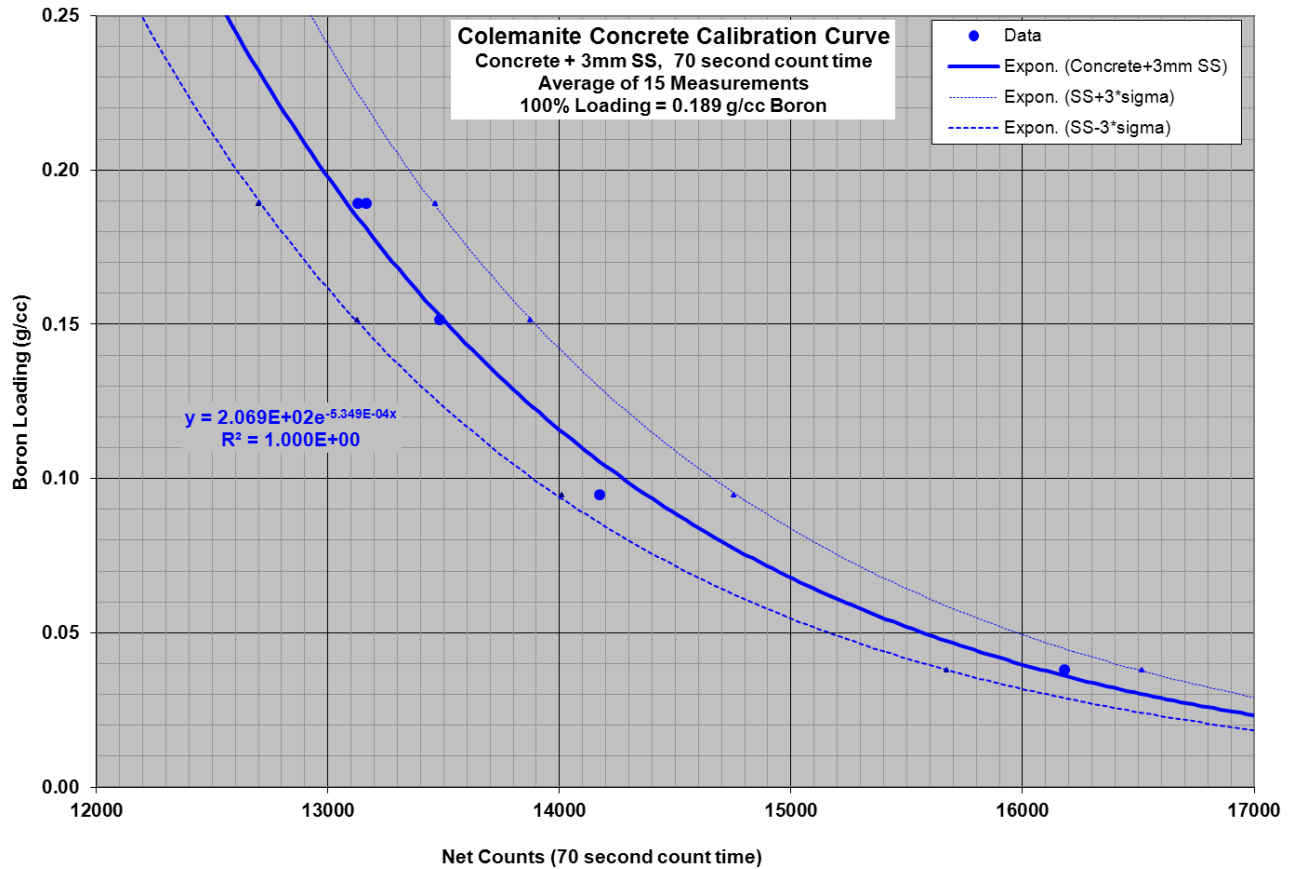


Figure 5. Stainless steel clad Colemanite concrete calibration curve.

Conclusion

We describe design, construction, and calibration of a fast neutron backscatter gauge using dual He-3 neutron detection. Results for the net backscatter detection rate in two counting configurations demonstrate the boron neutron absorption content and uniformity in facility process control concrete can be predicted with good precision in the range $0.001 \text{ g/cm}^3 < [B] < 0.250 \text{ g/cm}^3$.

References

1. Hamid Makil, Neutronic Inspection Report of Annular Panel: KPA TK9500_USA, October 1, 2008, LIST/DETECS/SSTM/RAP/08-048.
2. M. Basturk, J. Arzmann, W. Jerlich, N. Kardjilov, E. Lehmann, and M. Zawisky, **Journal of Nuclear Materials** 341 (2005) 189–200.
3. C. Murray Bartle, Chris Kroger, and John G. West, **Physica B**, 385–386 (2006) 927–929.
4. Turgay Korkut, Abdulhalik Karabulut, Gokhan Budak, Bunyamin Aygun, Osman Gencel, Aybaba Hancerliogullari, **Applied Radiation and Isotopes**, 70 (2012) 341–345.
5. Cheng-Si TSAO, Hung-Fa SHYU, Hsin-Fa FANG, Ming-Churng HSIEH and Shih-Chung CHENG, **Journal of Nuclear Science and Technology**, Vol. 43, No. 12, p. 1517–1521 (2006).
6. K. M. Gibbs and R. A. Dewberry, Invention Disclosure SRS-12-007, February 2012.
7. Hamid Tagziria, Neil J. Roberts, and David J. Thomas, **Nuclear Instruments and Methods in Physics Research Section A: Accelerators, Spectrometers, Detectors and Associated Equipment**, Volume 510, Issue 3, 2003, 346–356.
8. G. F. Knoll, **Radiation Detection and Measurement**, Third Edition, (John Wiley & Sons, 2000), page 511.
9. J. F. Breimeister, MCNP – A General Monte Carlo N-Particle Transport Code, LA-12625-M, Los Alamos Scientific Laboratory, 1993.
10. K. M. Gibbs, R. A. Dewberry, A. H. Couture, and S. Harris, “MOX Colemanite Concrete Neutron Gauge Calibration Inspection Report” SRNL-TR-2012-00001, January 2012.